Title
Further evidence of the Levantine Iron Age geomagnetic anomaly from Georgian pottery

Journal
Geophysical Research Letters, 44(5)

ISSN
0094-8276

Authors
Shaar, Ron
Tauxe, Lisa
Goguitchaichvili, Avto
et al.

Publication Date
2017-03-16

DOI
10.1002/2016gl071494

Further evidence of the Levantine Iron Age geomagnetic anomaly from Georgian pottery

Ron Shaar[1]*, Lisa Tauxe[2], Avto Goguitchaichvili[3], Marina Devidze[4-6], Vakhtang Licheli[5]

[1] The Institute of Earth Sciences, The Hebrew University of Jerusalem, Jerusalem 91904, Israel.

[2] Scripps Institution of Oceanography, University of California San Diego, La Jolla, CA 92093-0220, USA

[3] Laboratorio Interinstitucional de Magnetismo Natural, Instituto de Geofisica, UNAM, Morelia, Mexico

[4] M. Nodia Institute of Geophysics, Ivane Javakhishvili Tbilisi State University, Tbilisi, Georgia

[5] Institute of Archeology, Ivane Javakhishvili Tbilisi State University, Georgia

[6] Institute of Geoscience and Earth Resources (IGG-CNR), Italian National Research Council (CNR), Pisa, Italy

* Corresponding author: first and last name (ron.shaar@mail.huji.ac.il)

Key Points:

- Paleointensity data from Georgia from the past five millennia.
- High field values (145-154 ZAm^2) in Georgia in the 10^{th} century BCE
- New geographic constraints for the Levantine Iron Age geomagnetic Anomaly (LIAA)

(The above elements should be on a title page)

This article has been accepted for publication and undergone full peer review but has not been through the copyediting, typesetting, pagination and proofreading process which may lead to differences between this version and the Version of Record. Please cite this article as doi: 10.1002/2016GL071494

Abstract

Recent archaeomagnetic data from ancient Israel revealed the existence of a so-called "Levantine Iron Age geomagnetic anomaly" (LIAA) which spanned the first 350 years of the first millennium BCE and was characterized by a high averaged geomagnetic field (Virtual Axial Moment, VADM > 140 ZAm^2, nearly twice of today's field), short decadal-scale geomagnetic spikes (VADM of 160-185 ZAm^2), fast field variations, and substantial deviation from dipole field direction. The geographic constraints of the LIAA have remained elusive due to limited high quality paleointensity data in surrounding locations. Here, we report archaeointensity data from Georgia showing high field values (VADM > 150 ZAm^2) in the 10th or 9th century BCE, low field values (VADM < 60 ZAm^2) in the 12th century BCE, and fast field variation in the 5th and 4th centuries BCE. High field values in the timeframe of LIAA have been observed so far only in three localities near the Levant: Eastern Anatolia, Turkmenistan, and now Georgia, all located east of longitude 30E. West of this, in the Balkans, field values in the same time are moderate to low. These constraints put geographic limits on the extent of the LIAA, and support the hypothesis of an unusually intense regional geomagnetic anomaly during the beginning of the first half of the first millennium BCE, comparable in area and magnitude (but of opposite sign) to the presently active South Atlantic Anomaly.

1. Introduction

Detailed mapping of secular (short-term) variation of the geomagnetic field provides an essential indirect view into the geodynamics and thermal structure of Earth's core [*Jackson and Finlay*, 2007]. Thus, a substantial effort has been made over the last several decades to reconstruct past secular variations, with particular focus on the recent several centuries [*Finlay et al*., 2010; *Finlay et al*., 2016; *Jackson et al*., 2000] and more broadly, the Holocene [*Constable et al*., 2016; *Korte et al*., 2011]. Perhaps the most remarkable secular variation feature in this time window is the presently active regional negative geomagnetic anomaly over the southern Atlantic presumably driven by a reversed core flux patch [*Jackson et al*., 2000; *Tarduno et al*., 2015]. Until recently, there was no evidence for other historical geomagnetic anomalies of this scale. Recently, *Shaar et al*. [2016] proposed the existence of an intense positive geomagnetic anomaly over the Levant in the beginning of the first millennium BCE. This so-called "Levantine Iron Age Anomaly" (LIAA) is characterized by 350 years (ca. 1050 BCE – ca. 700 BCE) with high time-averaged field corresponding to

Virtual Axial Dipole Moment (VADM, [*Barbetti et al*., 1977; *Tauxe et al*., 2016a]) of about 140 ZAm^2 (nearly twice today's axial dipole moment, 76 ZAm^2). During this period of generally high field, at least two geomagnetic "spikes" (defined by *Cai et al*. [2014] as a short lived feature with a VADM of >160 ZAm^2) occurred in the 10th and the 8th centuries BCE reaching VADMs of 160-187 ZAm^2 ZAm^2 [*Ben-Yosef et al*., 2017; *Shaar et al*., 2011; *Shaar et al*., 2016] and perhaps even higher [*Ben-Yosef et al*., 2009]. The maximum directional deviations from axial dipole field direction in the LIAA period was at least 22° [*Shaar et al*., 2016]. The dataset supporting the LIAA hypothesis include 70 high-precision paleointensity estimates from well-dated pottery, burnt structures, and radiocarbon-dated slag [*Ben-Yosef et al*., 2009; *Ertepinar et al*., 2012; *Shaar et al*., 2011; *Shaar et al*., 2016] and directional data from in-situ cooking ovens [*Hassul et al*., 2016; *Shaar et al*., 2016]. To uncover the geographic extent of this anomaly, similarly dense high quality data from the narrow time window of LIAA are required from nearby locations.

Accurate recovery of ancient geomagnetic field intensity (paleointensity) is not a straightforward task. It requires well-dated materials carrying a stable thermoremenent magnetization (TRM) held by sub-micrometer scale single-domain (SD) or small (flower state) pseudo single domain (PSD) ferromagnetic particles, which are chemically resistant to repeated heating lab treatments [*Tauxe and Yamazaki*, 2007]. In the so-called 'Thellier' procedure, the ancient TRM acquired in an unknown field is gradually replaced with laboratory TRM acquired in a known field through multiple heating steps at progressively elevated temperatures [*Aitken et al*., 1988; *Coe*, 1967; *Thellier and Thellier*, 1959; *Yu et al*., 2004]. It is a laborious, time consuming, experimental procedure with a relatively low rate of success [*Tauxe and Yamazaki*, 2007; *Valet*, 2003] resulting from non-SD materials and experimental complexities. The interpretations of the experimental results, expressed as Arai plots [*Nagata et al*., 1963] and Zijderveld plots [*Zijderveld*, 1967] (Figure 1) can be non-unique and ambiguous. Thus, acceptance criteria based on paleointensity statistics [*Paterson et al*., 2014] are commonly applied to screen out unreliable interpretations. Additional uncertainties arise from remanence anisotropy [*Rogers et al*., 1979] and cooling-rate dependency of TRM [*Fox and Aitken*, 1980], which result in a typical bias of non-corrected paleointensity calculation of 5-25% [*Genevey and Gallet*, 2002; *Genevey et al*., 2008; *Shaar et al*., 2016], and in many cases even more than that.

Considering the above methodological complexities, it may not be surprising that some regional paleointensity datasets derived using different experimental methods, data interpretation guidelines, averaging schemes, and dating techniques can show considerable inconsistency and internal discrepancies [*Genevey et al*., 2008; *Pavon-Carrasco et al*., 2014]. If the raw measurements are in hand, then this problem can be partly addressed by carefully assembling regional compilations using identical laboratory and data analysis procedures. Two examples from the near east adopting such approach are the Levantine compilation [*Shaar et al*., 2016] that applies an automatic consistent interpretation routine [*Shaar and Tauxe*, 2013; *Shaar et al*., 2015] using strict acceptance criteria on the entire raw measurement data, and the Bulgarian compilation [*Kovacheva et al*., 2009; *Kovacheva et al*., 2014], which is based on the same lab treatments throughout the dataset. When the raw measurement data are unavailable, it is critical to screen out less reliable data using paleointensity statistics [*Genevey et al*., 2008; *Paterson et al*., 2014; *Pavon-Carrasco et al*., 2014] or other methods. This approach has been recently used by *Pavon-Carrasco et al*. [2014] who demonstrated the strong effect of quality criteria on regional geomagnetic modelling in Europe.

In this study we focus on the paleointensity behavior in Georgia in an effort to explore differences between the Levant and Georgia, located approximately 3000 km apart. The Caucasus was extensively studied in the 1970s and 1980s. The raw data from these publications are unavailable, but the published interpretations are available from the geomagia50 [*Brown et al*., 2015; *Korhonen et al*., 2008] and the MagIC (https://earthref.org/) databases. Adequate analysis of the published data should take into consideration possible bias caused by data quality. Thus, following *Pavon-Carrasco et al*. [2014] we show in gray circles in Figure 2, data derived using some form of the Thellier method. Data points in blue are derived using the Thellier method with pTRM checks and at least 4 specimens. The latter criterion is necessary to average anisotropy effects. The high values in Georgian dataset in the beginning of the first half of the first millennium BCE, with field values corresponding to geomagnetic spikes (VADM ~ 160 Z Am^2) are the main focus of this study. As these data were not obtained using the strict standards of modern studies, we provide here new paleointensity data from archaeologically dated potsherds and baked-clays in order to test the trend seen in the old data, and compare the behavior in the Caucasus and the Levant.

2. Methods

Forty eight potsherds and fired clay samples from different archaeological contexts, mostly dated using archaeological correlations [*Djibladze*., 2002; *Heinch and Kuntner*., 2016; *Licheli*, 2011; *Licheli and Rusishvili*, 2008; *Muskhelishvili*, 1978; *Narimanishvili*, 1991; *Pitskhelauri*, 1976] were analyzed in the paleomagnetic laboratory of Scripps Institution of Oceanography, University of California San Diego. A detailed information of the archaeological contexts can be found in the supporting information (Supporting Information, Appendix I). The samples were cut into 3-9 specimens, which were subjected to Thellier-type paleointensity experiment using the IZZI protocol of *Tauxe and Staudigel* [2004] including routine pTRM checks [*Coe et al*., 1978] at every second temperature step. Anisotropy of TRM was measured in six positions in 600° with additional baseline zerofield and alteration-check steps at the beginning and the end of the experiment, respectively. Cooling rate dependency was measured from three acquisitions of TRM in 600° cooled in fast air cooling (43 °/min), slow spontaneous cooling (1.3°/min), and fast cooling as alteration check (43 °/min), respectively. Following *Shaar et al*. [2016] we assumed an averaged ancient cooling time of 6 hours from 500° to 200° for all the archaeological samples (0.83 °/min). Data analysis was done using the Thellier GUI program [*Shaar and Tauxe*, 2013], part of the PmagPy software [*Tauxe et al*., 2016b]. We use the automatic interpretation technique [*Shaar and Tauxe*, 2013; *Shaar et al*., 2015] using the acceptance criteria listed in Table 1. The error bounds of the paleointensity estimates were calculated from two parameters: the standard deviation of the mean (σ) and the “extended error” [*Shaar et al*., 2016]. The latter takes into consideration all possible interpretations passing the criteria. Additional details regarding procedures and analyses can be found in *Shaar et al*. [2016].

3. Results

Figure 1 shows representative behaviors in the paleointensity experiments. Figures 1a-c show different examples of specimens with behaviors failing one or more of the acceptance criteria in Table 1. Figure 1d shows the behavior of a nearly ideal specimen with a straight Arai plot, no evidence of alteration and a straight Zijderveld plot converging to the origin (insets); this specimen passed all criteria. The effect of cooling rate is illustrated in Figure 1e, following Figure 4 in *Halgedahl et al*. [1980], where the TRM overestimation is plotted versus the logarithm of the ratio of cooling rates.

Overall, 91 specimens out of 210 specimens passed the specimen level criteria (43% success rate), and 17 samples out of 48 passed the sample criteria (35% success rate). The samples' paleointensities are listed in Table 2 and shown in Figure 2 as red squares. Histograms showing distributions of statistics, and cooling rate and anisotropy corrections are given in the Supporting Information. Interpretations in the specimens and sample level with the corresponding statistical data, and the entire set of raw measurements are available in the MagIC database (http://earthref.org/MagIC/11631).

Four locations yielded 2-3 samples per age interval: Khovle, and Atskuri that show good internal consistency, and Graklinai Gora and Tsminda Pchani that show more scattered results. We note the relatively large uncertainty in the archaeological context of the samples from Graklinai Gora (Supporting Information, Appendix I). We suggest that the source of the scatter in Graklinai Gora is fast variation rate between the 5th and the 3rd centuries BCE. This hypothesis is supported by the previous data that show a wide range of values in the 500 BCE to 200 BCE interval (Figure 2). Some of the locations yielded single samples per time interval; although passing our strict selection criteria, these time intervals should be further confirmed by more data.

The new data shown in Figure 2 corroborate the main trends seen in the old data. Most importantly, they show the following features:

- High geomagnetic field (VADM of 145 - 154 Z Am^2) in the 9th or 10th century BCE, supported by three samples from Khovle.
- Geomagnetic low in the 14th or 13th century BCE with VADMs < 60 Z Am^2, supported by two samples from Tsminda Pchani and Ortsheni necropolis.
- Large scatter in the data in the 5th and 4th century BCE with 8 samples from Tsminda Pchani, Grakliani Gora and Grakliani Hill showing VADMs ranging between 80 – 140 Z Am^2. Also, one sample from Grakliani Hill yielded anomalously low value (50 Z Am^2) that needs to be confirmed by more samples. This could be explained by fast field variations or age uncertainty. As age uncertainty of few hundred years in these sites is unlikely, we interpret the scatter as a period with fast field variations.

4. Discussion

Three samples from the Iron Age site of Khovle showed high VADM values of 145 – 154 ZAm^2 around 900 BCE. Considering the extended error bounds (Table 2), these values are slightly lower than the Levantine geomagnetic spikes values (> 160 ZAm^2), but comparable in magnitude. Some of the published Caucasus data also show high field values in this period (Figure 2), with three samples showing VADMs of about 160 ZAm^2 around 800 BCE and a few quite high values (>160 ZAm^2) coming from pottery from the second millennium BCE; however these do not meet the criteria of *Pavon-Carrasco et al*. [2014]. Our new high values thus confirm the existence of a paleointensity high around 900 BCE in Georgia. The picture is not so simple, however. There is a large dispersion of data in the 1000 BCE - 800 BCE interval with field values ranging from 50 Z Am^2 to 150 ZAm^2. Evidently, more-high quality well-dated data are required to fully characterize field variations in this period. The 900 BCE high in Georgia is contemporaneous with the Levantine geomagnetic spikes, suggesting a link between the Levant and Caucasus. Both locations show fast field variations and exceptionally high field values. We conclude, therefore, that the LIAA extended at least to Georgia. Yet, still, more data is required to understand the details of the LIAA evolution in the Caucasus.

With the new data in hand it is now possible to inspect the overall evidences for the geographic extent of the LIAA using the available paleointensity data from nearby localities (Figure 3). We display regional compilations outside the Levant using two sets of criteria: data obtained using the Thellier method in gray symbols, and data passing *Pavon-Carrasco et al*. [2014] criteria (Thellier-type methods with pTRM check and at least four specimens) in colored symbols. The Levantine paleointensity behavior, to which we compare the Georgian data, is shown in the south west corner of the map in Figure 3, consisting of the Central Levant data in red [*Ben-Yosef et al*., 2017; *Ben-Yosef et al*., 2009; *Shaar et al*., 2011; *Shaar et al*., 2015; *Shaar et al*., 2016] (analyzed and interpreted using identical methods and selection criteria), and from Syria and Turkey in cyan [*Ertepinar et al*., 2012; *Gallet and Butterlin*, 2015; *Gallet et al*., 2006; *Gallet et al*., 2008; *Gallet et al*., 2014; *Gallet et al*., 2015; *Genevey et al*., 2003; *Stillinger et al*., 2015]. The LIAA period with the two spikes is highlighted by a shaded orange stripe. The Bulgarian dataset, compiled by *Kovacheva et al*. [2009] and *Kovacheva et al*. [2014], provides a detailed paleointensity picture, but has only a few samples covering the first half of the first millennium BCE; this data set shows low to moderate values during the LIAA. The Greek dataset, available from the GEOMAGIA50 and MagIC databases, with the revisions of *Tema and Kondopoulou* [2011] and *Tema et al*. [2012], also shows a paleointensity low during LIAA. From these data it seems that there was no paleointensity high in the Balkan during the LIAA, and thus, the Balkans mark its western limit. East of the Caucasus, the Turkmenistan dataset assembled using data available from the GEOMAGIA50 and MagIC databases, show a coherent paleointensity behavior with similar trends as the Levant and Georgia, and high field values corresponding to VADM of at least 150 ZAm^2. Yet, we note that these data do not meet *Pavon-Carrasco et al*. [2014] criteria, and thus shown in gray. We conclude that the LIAA extended from the Levant toward western Asia.

Inspection of the regional data in Figure 3 shows two prominent peaks. The first of which is the LIAA east of the Balkans shown with orange stripe and discussed above. The second peak appears to be contemporaneous in all locations of the near east, and is highlighted with green stripe. It reached values of 150 – 160 ZAm^2 in Georgia, Bulgaria and Greece, 140 Zam^2 in the Levant, and possibly more than 160 Zam^2 in Turkmenistan (need to be confirmed by higher quality data). This peak has been observed and discussed in *Tema and Kondopoulou* [2011] and *Pavon-Carrasco et al*. [2014], and is associated with period of relatively fast secular variation in Europe. Also here, further data is needed to adequately describe the spatial and temporal characteristics of this second peak.

5. Conclusions

From comparison of paleointensity datasets from the Balkan, Caucasus, Levabt, and Turkmenistan we conclude that a non-dipole feature is required to explain the paleointensity difference in the interval between 1050 BCE to 700 BCE between Caucasus-Levant and the Balkans. We suggest that this non-dipole feature is the regional positive geomagnetic anomaly suggested by *Shaar et al*. [2016]. Given the new high Georgian paleointensity data in the 10^{th} or 9^{th} century BCE we conclude that the western limit of the Levantine Iron-Age Anomaly (LIAA) is along longitude lines of about 30E – 35E.

Acknowledgments

We thank Manuel Calvo Rathert for his assistance in the field work. We thank Jason Steindorf for helping with the laboratory measurements. This project was supported by UC Mexus grant # CN-09-282 to LT and AG, NSF grant # EAR 1345003 to LT and the Israel Science Foundation grant No. 1364/15 to RS. We are very grateful for two excellent anonymous reviews which substantially improved the quality of the manuscript.

The data and interpretations associated with this publication are available from the MagIC database in http://earthref.org/MagIC/11631

References

Aitken, M. J., A. L. Allsop, G. D. Bussell, and M. B. Winter (1988), Determination of the Intensity of the Earths Magnetic-Field during Archaeological Times - Reliability of the Thellier Technique, *Rev Geophys*, *26*(1), 3-12.

Barbetti, M. F., M. W. Mcelhinny, D. J. Edwards, and P. W. Schmidt (1977), Weathering Processes in Baked Sediments and Their Effects on Archeomagnetic Field-Intensity Measurements, *Phys Earth Planet In*, *13*(4), 346-354.

Ben-Yosef, E., M. Milman, R. Shaar, L. Tauxe, and O. Lipschits (2017), Seven centuries of geomagnetic intensity variations recorded by royal Judean stamped jar handles, *Proceedings of the National Academy of Sciences*, *in press*.

Ben-Yosef, E., L. Tauxe, T. E. Levy, R. Shaar, H. Ron, and M. Najjar (2009), Geomagnetic intensity spike recorded in high resolution slag deposit in Southern Jordan, *Earth Planet Sc Lett*, *287*(3-4), 529-539.

Brown, M. C., F. Donadini, A. Nilsson, S. Panovska, U. Frank, K. Korhonen, M. Schuberth, M. Korte, and C. G. Constable (2015), GEOMAGIA50.v3: 2. A new paleomagnetic database for lake and marine sediments, *Earth Planets and Space*, *67*.

Cai, S. H., L. Tauxe, C. L. Deng, Y. X. Pan, G. Y. Jin, J. M. Zheng, F. Xie, H. F. Qin, and R. X. Zhu (2014), Geomagnetic intensity variations for the past 8 kyr: New archaeointensity results from Eastern China, *Earth Planet Sc Lett*, *392*, 217-229.

Coe, R. S. (1967), Paleo-intensities of Earths magnetic field determined from Tertiary and Quaternary rocks, *Journal of Geophysical Research*, *72*(12), 3247-3262.

Coe, R. S., S. Gromme, and E. A. Mankinen (1978), Geomagnetic paleointensities from radiocarbon-dated lava flows on hawaii and question of pacific nondipole low, *Journal of Geophysical Research*, 1740-1756.

Constable, C., M. Korte, and S. Panovska (2016), Persistent high paleosecular variation activity in southern hemisphere for at least 10 000 years, *Earth Planet Sc Lett*, *453*, 78-86.

Ertepinar, P., C. G. Langereis, A. J. Biggin, M. Frangipane, T. Matney, T. Okse, and A. Engin (2012), Archaeomagnetic study of five mounds from Upper Mesopotamia between 2500 and 700 BCE: Further evidence for an extremely strong geomagnetic field ca. 3000 years ago, *Earth Planet Sc Lett*, *357*, 84-98.

Finlay, C. C., M. Dumberry, A. Chulliat, and M. A. Pais (2010), Short Timescale Core Dynamics: Theory and Observations, *Space Science Reviews*, *155*(1-4), 177-218.

Finlay, C. C., N. Olsen, S. Kotsiaros, N. Gillet, and L. Toffner-Clausen (2016), Recent geomagnetic secular variation from Swarm and ground observatories as estimated in the CHAOS-6 geomagnetic field model, *Earth Planets and Space*, *68*.

Fox, J. M. W., and M. J. Aitken (1980), Cooling-rate dependence of thermoremanent magnetization, *Nature*, *283*(5746), 462-463.

Gallet, Y., and P. Butterlin (2015), Archaeological and Geomagnetic Implications of New Archaeomagnetic Intensity Data from the Early Bronze High Terrace "Massif Rouge' at Mari (Tell Hariri, Syria), *Archaeometry*, *57*, 263-276.

Gallet, Y., A. Genevey, M. Le Goff, F. Fluteau, and S. A. Eshraghi (2006), Possible impact of the Earth's magnetic field on the history of ancient civilizations, *Earth Planet Sc Lett*, *246*(1-2), 17-26.

Gallet, Y., M. Le Goff, A. Genevey, J. Margueron, and P. Matthiae (2008), Geomagnetic field intensity behavior in the Middle East between similar to 3000 BC and similar to 1500 BC, *Geophysical Research Letters*, *35*(2).

Gallet, Y., M. D'Andrea, A. Genevey, F. Pinnock, M. Le Goff, and P. Matthiae (2014), Archaeomagnetism at Ebla (Tell Mardikh, Syria). New data on geomagnetic field intensity variations in the Near East during the Bronze Age, *Journal of Archaeological Science*, *42*, 295-304.

Gallet, Y., M. M. Montana, A. Genevey, X. C. Garcia, E. Thebault, A. G. Bach, M. Le Goff, B. Robert, and I. Nachasova (2015), New Late Neolithic (c. 7000-5000 BC) archeointensity data from Syria. Reconstructing 9000 years of archeomagnetic field intensity variations in the Middle East, *Phys Earth Planet In*, *238*, 89-103.

Genevey, A., and Y. Gallet (2002), Intensity of the geomagnetic field in western Europe over the past 2000 years: New data from ancient French pottery, *Journal of Geophysical Research-Solid Earth*, *107*.

Genevey, A., Y. Gallet, C. G. Constable, M. Korte, and G. Hulot (2008), ArcheoInt: An upgraded compilation of geomagnetic field intensity data for the past ten millennia and its application to the recovery of the past dipole moment, *Geochem Geophy Geosy*,DOI 10.1029/2007GC001881, -.

Genevey, A. S., Y. Gallet, and J. C. Margueron (2003), Eight thousand years of geomagnetic field intensity variations in the eastern Mediterranean, *Journal of Geophysical Research-Solid Earth*, *108*(B5).

Halgedahl, S. L., R. Day, and M. Fuller (1980), The Effect of Cooling Rate on the Intensity of Weak-Field Trm in Single-Domain Magnetite, *Journal of Geophysical Research*, *85*(Nb7), 3690-3698.

Hassul, E., R. Shaar, A. Agnon, N. N., and I. Finkelstein (2016), Archaeomagnetic directions from burnt structures in Tel Megiddo, in *Megiddo VI*, edited, Tel-Aviv University, Tel Aviv.

Jackson, A., and C. C. Finlay (2007), Geomagnetic secular variation and its applications to the core, in *Treatise on Geophysics*, edited by K. M, pp. 147–193, Elsevier, New York.

Jackson, A., A. R. T. Jonkers, and M. R. Walker (2000), Four centuries of geomagnetic secular variation from historical records, *Philosophical Transactions of the Royal Society of London Series a-Mathematical Physical and Engineering Sciences*, *358*(1768), 957-990.

Kirschvink, J. (1980), The least-squares line and plane and the analysis of paleomagnetic data, *Geophysical Journal of the Royal Astronomical Society*, 699-718.

Korhonen, K., F. Donadini, P. Riisager, and L. J. Pesonen (2008), GEOMAGIA50: An archeointensity database with PHP and MySQL, *Geochem Geophy Geosy*, *9*.

Korte, M., C. Constable, F. Donadini, and R. Holme (2011), Reconstructing the Holocene geomagnetic field, *Earth Planet Sc Lett*, *312*(3-4), 497-505.

Kovacheva, M., Y. Boyadziev, M. Kostadinova-Avramova, N. Jordanova, and F. Donadini (2009), Updated archeomagnetic data set of the past 8 millennia from the Sofia laboratory, Bulgaria, *Geochem Geophy Geosy*, *10*.

Kovacheva, M., M. Kostadinova-Avramova, N. Jordanova, P. Lanos, and Y. Boyadzhiev (2014), Extended and revised archaeomagnetic database and secular variation curves from Bulgaria for the last eight millennia, *Phys Earth Planet In*, *236*, 79-94.

Nagata, T., Y. Arai, and K. Momose (1963), Secular variation of the geomagnetic total force during the last 5000 years, *Journal of Geophysical Research*, *68*, 5277-5282.

Paterson, G. A., L. Tauxe, A. J. Biggin, R. Shaar, and L. C. Jonestrask (2014), On improving the selection of Thellier-type paleointensity data, *Geochem Geophy Geosy*, *15*(4), 1180-1192.

Pavon-Carrasco, F. J., M. Gomez-Paccard, G. Herve, M. L. Osete, and A. Chauvin (2014), Intensity of the geomagnetic field in Europe for the last 3 ka: Influence of data quality on geomagnetic field modeling, *Geochem Geophy Geosy*, *15*(6), 2515-2530.

Rogers, J., J. M. W. Fox, and M. J. Aitken (1979), Magnetic anisotropy in ancient pottery, *Nature*, *277*(5698), 644-646.

Selkin, P. A., and L. Tauxe (2000), Long-term variations in palaeointensity, *Philosophical Transactions of the Royal Society of London Series a-Mathematical Physical and Engineering Sciences*, *358*(1768), 1065-1088.

Shaar, R., and L. Tauxe (2013), Thellier GUI: An integrated tool for analyzing paleointensity data from Thellier-type experiments, *Geochem Geophy Geosy*, *14*(3), 677-692.

Shaar, R., E. Ben-Yosef, H. Ron, L. Tauxe, A. Agnon, and R. Kessel (2011), Geomagnetic field intensity: How high can it get? How fast can it change? Constraints from Iron-Age copper-slag, *Earth Planet Sc Lett*, *301*, 297–306.

Shaar, R., L. Tauxe, E. Ben-Yosef, V. Kassianidou, B. Lorentzen, J. M. Feinberg, and T. E. Levy (2015), Decadal-scale variations in geomagnetic field intensity from ancient Cypriot slag mounds, *Geochem Geophy Geosy*, *16*(1), 195-214.

Shaar, R., L. Tauxe, H. Ron, Y. Ebert, S. Zuckerman, I. Finkelstein, and A. Agnon (2016), Large geomagnetic field anomalies revealed in Bronze to Iron Age archeomagnetic data from Tel Megiddo and Tel Hazor, Israel, *Earth Planet Sc Lett*, *442*, 173-185.

Stillinger, M. D., J. M. Feinberg, and E. Frahm (2015), Refining the archaeomagnetic dating curve for the Near East: new intensity data from Bronze Age ceramics at Tell Mozan, Syria, *Journal of Archaeological Science*, *53*, 345-355.

Tarduno, J. A., M. K. Watkeys, T. N. Huffman, R. D. Cottrell, E. G. Blackman, A. Wendt, C. A. Scribner, and C. L. Wagner (2015), Antiquity of the South Atlantic Anomaly and evidence for top-down control on the geodynamo, *Nature Communications*, *6*.

Tauxe, L., and H. Staudigel (2004), Strength of the geomagnetic field in the Cretaceous Normal Superchron: New data from submarine basaltic glass of the Troodos Ophiolite, *Geochem Geophy Geosy*,DOI 10.1029/2003GC000635, -.

Tauxe, L., and T. Yamazaki (2007), Paleointensities, in *Treatise on Geophysics* edited, pp. 509-563, Elsevier.

Tauxe, L., S. K. Banerjee, R. F. Butler, and R. Van der Voo (2016a), *Essentials of Paleomagnetism*, 4th Web Edition ed.

Tauxe, L., R. Shaar, L. Jonestrask, N. L. Swanson-Hysell, R. Minnett, A. A. P. Koppers, C. G. Constable, N. Jarboe, K. Gaastra, and L. Fairchild (2016b), PmagPy: Software package for paleomagnetic data analysis and a bridge to the Magnetics Information Consortium (MagIC) Database, *Geochem Geophy Geosy*, *17*(6), 2450-2463.

Tema, E., and D. Kondopoulou (2011), Secular variation of the Earth's magnetic field in the Balkan region during the last eight millennia based on archaeomagnetic data, *Geophysical Journal International*, *186*(2), 603-614.

Tema, E., M. Gomez-Paccard, D. Kondopoulou, and Y. Almar (2012), Intensity of the Earth's magnetic field in Greece during the last five millennia: New data from Greek pottery, *Phys Earth Planet In*, *202*, 14-26.

Thellier, E., and O. Thellier (1959), Sur l'intensité du champ magnétique terrestre dans le passé historique et géologique, *Ann*. *Geophys*., *15*, 285–376.

Valet, J. P. (2003), Time variations in geomagnetic intensity, *Rev Geophys*, *41*(1).

Yu, Y. J., L. Tauxe, and A. Genevey (2004), Toward an optimal geomagnetic field intensity determination technique, *Geochem Geophy Geosy*, *5*.

Zijderveld, J. D. A. (1967), AC demagnetization of rocks: analysis of results, in *Methods in paleomagnetism*, edited by D. W. Collinson, K. M. Creer and S. K. Runcorn, pp. 254–286, Elsevier, New York.

Table 1: Acceptance criteria

Criteria group	Statistic	Threshold value	Description	Reference [b]
Specimen paleointensity[a]	FRAC	0.79	Fraction parameter	(1)
	β	0.1	Scatter parameter	(2)
	SCAT	True	Scatter parameter	(1)
	N_{PTRM}	2	Number of pTRM checks	
	MAD	5	Maximum Angular Deviation of the zero field steps	(4)
	DANG	10	Deviation Angle	(5)
	Alteration check in correction protocols	5%	Alteration check in Non-Linear-TRM, TRM anisotropy, and cooling rate experiments	(6)
Sample paleointensity	N_{min}	3	Minimum number of specimens	
	σ	σ% < 10%	Standard deviation of the sample mean	
	$N_{min\_aniso\_corr}$	at least half of the specimens	Minimum number of specimens with anisotropy correction	(6)
	$N_{min\_cr\_corr}$	1	Minimum number of specimens with cooling rate correction	(6)
	sample anisotropy	1%	Minimum averaged anisotropy correction factor for excluding specimens with no anisotropy data	(6)

[a] For a complete description and definitions see Paterson et al. (2014) (http://www.paleomag.net/SPD/)

[b] (1):[*Shaar and Tauxe*, 2013]; (2): [*Coe et al*., 1978]; (3): [*Selkin and Tauxe*, 2000]; (4):[*Kirschvink*, 1980] ; (5) [*Tauxe and Staudigel*, 2004] ; (6) [*Shaar et al*., 2016]

Table 2: Sample paleointensiy

Location	Lat/Lon	Sample ID	Type	Age range (CE)	N	B ± σ (μT)	VADM± σ (ZAm^2)	B extended error bounds (μT)	VADM error bounds (ZAm^2)
Sachkhere	42.302,43.383	gsa101	Pot Sherd	-3000,-2500	6	47.0±1.4	79.1±2.3	40.9-45.6	68.8 -86.4
Tsminda Pchani	41.632,45.450	gtp202	Pot Sherd	-1400,-1200	4	35.1±3.5	59.5±5.9	31.6-31.6	53.6 -65.3
		gtp108	Pot Sherd	-500,-400	3	51.7±1.3	87.7±2.1	45.7-49.2	77.5-97.9
		gtp107	Pot Sherd	-500,-400	5	59.9±2.5	102.0±4.3	54.7-57.4	92.8-106.0
Ortsheni necropolis	42.010,44.785	gon102	Pot Sherd	-1300,-1200	3	30.7±2.5	51.9±4.2	27.3-28.2	46.2-57.8
Khovle	41.910,44.247	gkv102	Pot Sherd	-1000,-800	6	89.6±0.1	152.0±0.1	87.1-90.9	147.3-160.4
		gkv103	Pot Sherd	-1000,-800	5	86.0±0.7	145.0±1.1	82.7-85.2	139.8-150.2
		gkv101	Brick	-1000,-800	4	91.1±0.1	154.0±0.1	86.8-94.1	146.7-164.1
Grakliani gora	41.997,44.404	ggg301	Pot Sherd	-400,-500	5	76.9±7.3	130.0±12.4	69.6-69.6	117.6-142.3
		ggg202	Pot Sherd	-400,-350	5	85.3±0.2	144.0±0.3	82.3-85.8	139.1-150.6
		ggg102	Brick	-400,-350	4	62.6±1.6	106.0±2.6	56.1-61.9	94.8-117.3
		ggg101	Brick	-400,-350	5	79.6±5.1	134.0±8.6	67.5-73.8	114.0-147.9
Grakliani Hill	41.998,44.403	ggh201	Pot Sherd	-500,-350	4	31.5±1.2	53.2±2.1	28.8-30.7	48.6-59.5
		ggh401	Pot Sherd	-450,-350	6	71.4±0.1	121.0±0.1	66.8-73.3	112.9-129.9
		ggh501	Pot Sherd	-350,-250	6	55.0±2.6	92.9±4.4	50.6-52.9	85.4-99.7
Atskuri	41.728,43.166	gat104	Oven	1400,1500	3	48.6±0.2	82.4±0.4	47.5-48.4	80.5-83.6
		gat102	Oven	1400,1500	7	50.7±2.2	85.9±3.7	47.0-48.9	79.6-94.5

[a] Ages in brackets are inferred archaeological date range.

[b] Error bounds calculated using all interpretations passing criteria (see *Shaar et al*. [2016] for details)

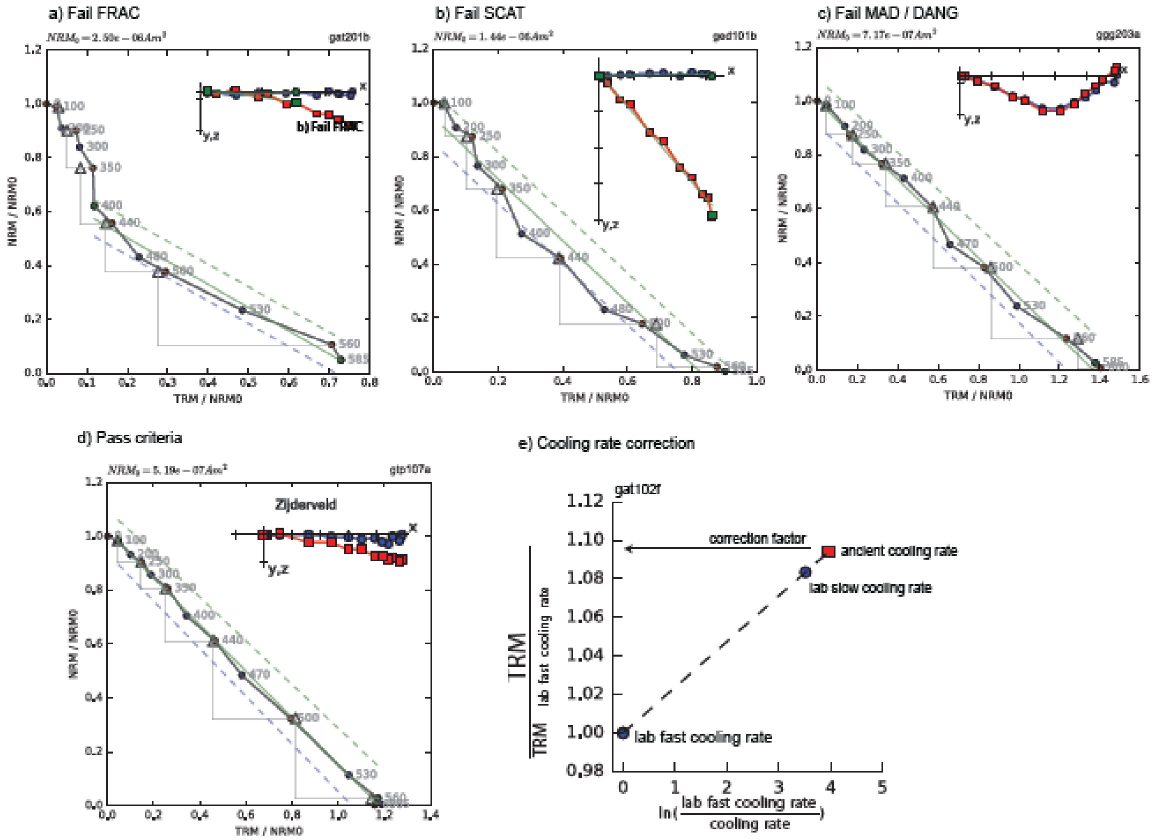

Figure 1: Representative behavior in paleointensity experiments. a-d) Arai plots where red circles, blue circles and triangles are ZI, IZ steps, and pTRM checks, respectively. Best-fit lines and SCAT boundaries are shown in green and dahed lines. Insets show Zijderveld plots where blue (red) squares are x–y (x–z) projections of the NRMs in specimens coordinate system (x-axis is rotated to the direction of the NRM). Interpretations failing criteria are shown in (a)-(c). Interpretation passing all criteria is shown in (d). e) cooling rate correction data plotted following Halgedahl et al. (1980).

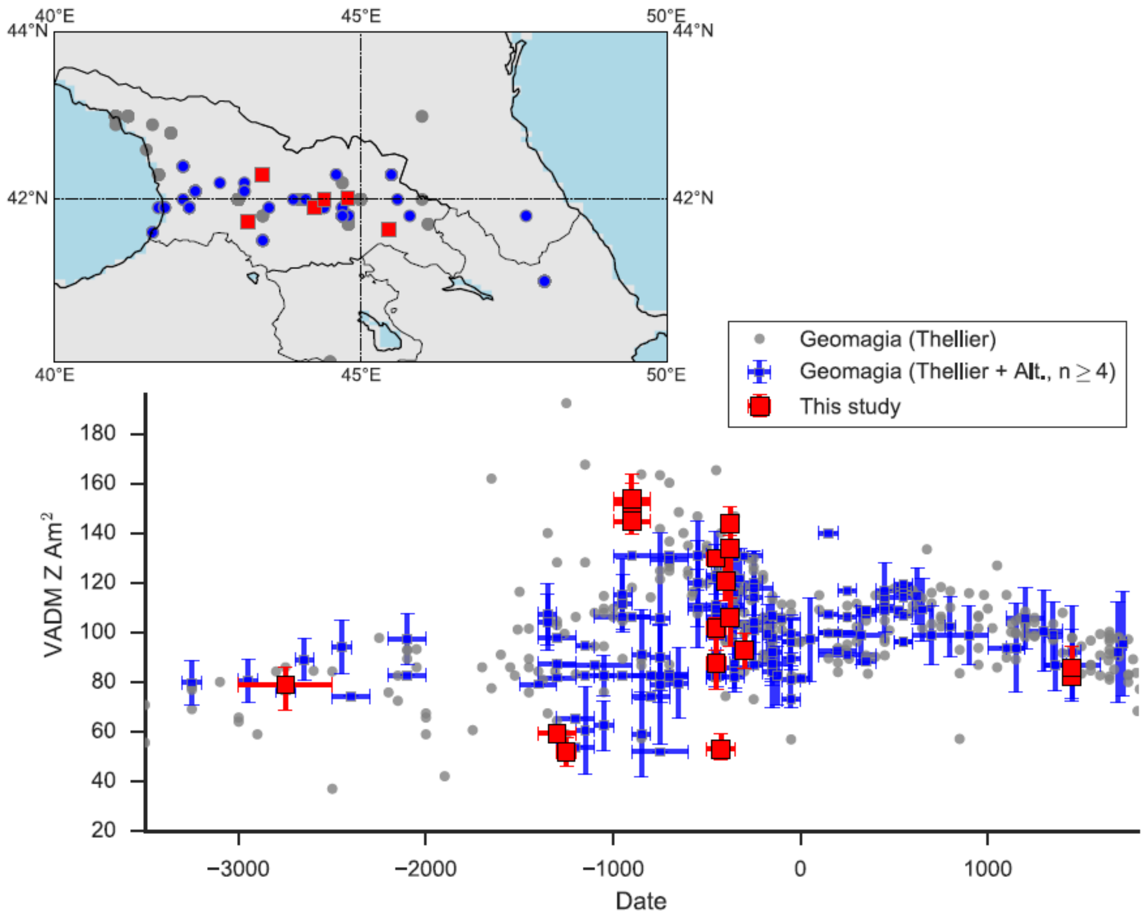

Figure 2: Paleointensity of the past 5000 years in the Caucasus displayed as VADM (Virtual Axial Dipole Moment). Red: This study; Gray: Thellier method data from GEOMAGIA50 database [*Brown et al*., 2015]; Blue: Thellier method with alteration check data from GEOMAGIA50 calculated using at least 4 specimens.

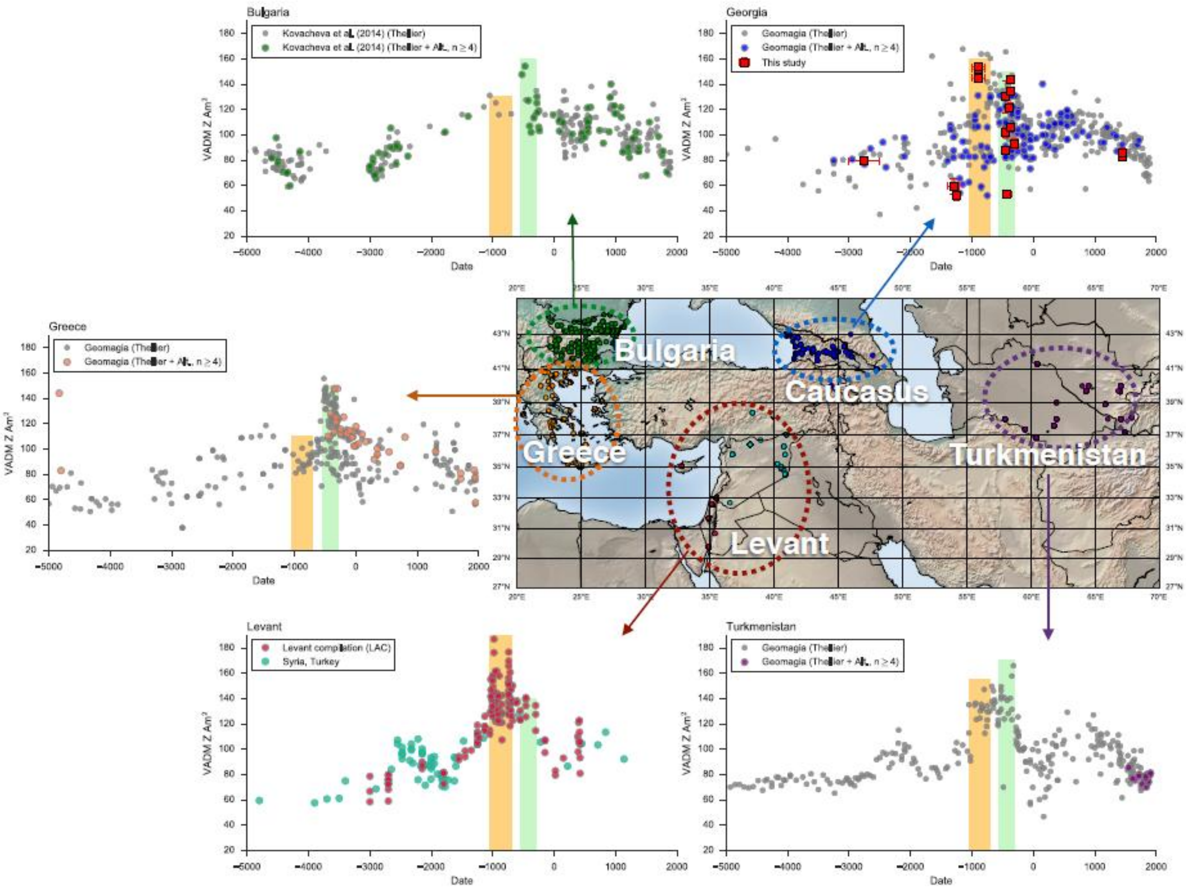

Figure 3: Regional compilations of paleointensity data from the Near East shown as Virtual Axial Diople moment (VADM). In the timeframe of the Levantine Iron Age Anomaly (LIAA, ca. 1050 BCE to ca. 700 BCE, highlighted in orange) there are prominent high VADM values in the Levant (160-185 ZAm^2), Caucasus (150 ZAm^2), and possibly Turkmenistan (~150 ZAm^2), but much lower values in Greece (<110 ZAm^2) and Bulgaria (<130 ZAm^2). In the period between 550 BCE and 250 BCE (highlighted in green), a second paleointensity high with VADM of 140-160 ZAm^2 (possibly higher in Turkmenistan) is observed in all regions.